**Natural Hazards
and Earth
System Sciences**

# Historical variation and trends in storminess along the Portuguese South Coast

**L. P. Almeida[1], Ó. Ferreira [1], M. I. Vousdoukas[1,4], and G. Dodet[2,3]**

[1]CIMA-Universidade do Algarve, Campus Gambelas, Faro, Portugal
[2]Faculdade de Ciências da Universidade Nova de Lisboa, Lisboa, Portugal
[3]Laboratório National de Engenharia Civil, Lisboa, Portugal
[4] Forschungszentrum Küste, Hannover, Germany

**Abstract.** This work investigates historical variation and trends in storm climate for the South Portugal region, using data from wave buoy measurements and from modelling, for the period 1952 to 2009. Several storm parameters (annual number of storms; annual number of days with storms; annual maximum and mean individual storm duration and annual 99.8th percentile of significant wave height) were used to analyse: (1) historical storminess trends; (2) storm parameter variability and relationships; and (3) historical storminess and its relationship to the North Atlantic Oscillation (NAO). No statistically significant linear increase or decrease was found in any of the storm parameters over the period of interest. The main pattern of storm characteristics and extreme wave heights is an oscillatory variability with intensity peaks every 7–8 yr, and the magnitude of recent variations is comparable with that of variations observed in the earlier parts of the record. In addition, the results reveal that the NAO index is able to explain only a small percentage of the variation in storm wave height, suggesting that more local factors may be of importance in controlling storminess in this region.

## 1 Introduction

The most dramatic and long-lasting meteorological impacts on many coasts are those resulting from storms (Schwartz, 2005). Due to its impact on socioeconomic structures and, in some cases, on human life, a storm climate attracts public attention and presents problems for coastal managers who need to understand the potential risk as a basis for decision-making.

The North Atlantic Ocean has been the focus of a number of studies aimed at assessing storm climate trends, with the majority focused on the northern part of the ocean. Most of the studies point towards an increase in storminess and in mean significant wave height between 1953 and 2009 (Bacon and Carter, 1991; Wang and Swail, 2001; Alexander et al., 2005; Grigorieva and Gulev, 2006; Dodet et al., 2010), as well as in cyclonic activity (Serreze et al., 1997; Geng and Sugi, 2001; Gulev et al., 2001; Wang et al., 2006). There are exceptions to these estimates, such as the cases of Dolan et al. (1989), WASA (1998), and Ferreira et al. (2009), who concluded that there has been no significant trend in the level of storminess between 1942 and 2009. However, there is a clear cyclic behaviour of storminess and wave height variability, on a decadal timescale (WASA, 1998).

The central and southern latitudes of the North Atlantic have been less well studied than the northern parts and, in general, the estimates of storm and wave climates for these latitudes have been derived from larger scale studies of the entire North Atlantic. Despite the different periods of analysis, most of these studies indicate a similar pattern in the multi-decadal variability in extreme and mean significant wave heights. The pattern indicates that the northern part of the North Atlantic presents a trend of increasing storminess and mean significant wave height, and that the mid and southern latitudes show a decreasing trend (Kushnir et al., 1997; Wang and Swail, 2000; Swail et al., 2000; Wang et al., 2003; Dodet et al., 2010). Although such larger-scale studies are useful in order to produce a more comprehensive interpretation of the overall pattern of variability in storminess, site-specific studies are required, particularly in locations where the specific site characteristics (e.g. local wind forcing and coastal physiography) can produce divergent trends. As an example, the European-funded Micore project (www.micore.eu) developed a study that integrated 12 independent and site-specific historical storminess
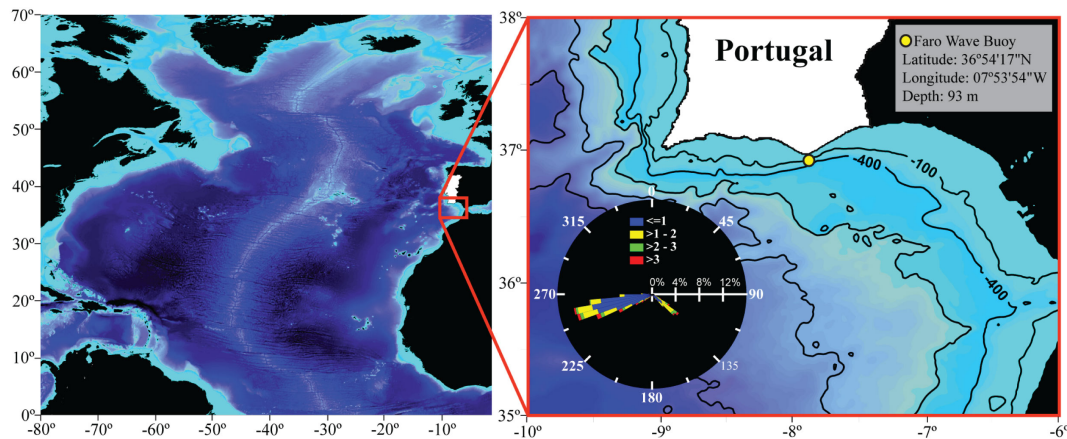
**Fig. 1.** The study area, including the location of the Faro buoy (the same as the simulated wave model point) and the wave rose distribution for the measured data.

analyses from several European regions. The main conclusion derived from that study is that a clear trend of change in storminess at a European-wide level is not evident. The results reveal a wide variability in trends between different coastal regions (Ferreira et al., 2009).

The south of Portugal is a region sheltered from the most dominant and important swell source, the North Atlantic. Besides the long travel distance involved, storms generated in the North Atlantic have to circumvent the southern Portuguese continental shelf to reach the coast. These factors contribute to an important dissipation of storm energy and wave height, which can consequently introduce different patterns into storm variability. The local storm wave climate is also influenced from the southeast by stormy waves originating in the Gibraltar Strait region (Levante storms). These aforementioned site-specific characteristics and their possible effect on storminess provide the motivation for the development of a detailed investigation into historical trends in storm wave climate for the south of Portugal. This investigation uses both modelling efforts and wave buoy measurements to assess changes in storminess, and compares the results with those of previous studies. In addition, the relationship between historical storminess and variation in the NAO index is determined, in an effort to understand the ability of this index to explain the pattern of storms in South Portugal.

## 2 Wave dataset

Wave data used in this study were obtained from two distinct sources covering different periods: for the period May 1995 to December 2009, measured data were obtained from a directional wave buoy (Faro buoy, from the Portuguese Hydrographical Institute – IH); and for the period January 1952 to February 1994, modelled data were obtained from a regional model hindcast implemented for the present purpose. Both series have an identical geographical origin located in

the middle latitudes of the North Atlantic, near the southern coast of Portugal (Fig. 1). The measured data and validated modelled data were joined to create a wave dataset covering a period of 57 yr from January 1952 to December 2009.

### 2.1 Measured data and wave climate

Recorded three-hourly values of significant wave height ($H_s$), mean peak period ($T$), and mean wave direction ($\theta$) were gathered from Faro buoy ($7°53'54''$ W ; $36°54'7''$ N), which is located off Cape Santa Maria at approximately 93 m water depth (Fig. 1). The measured data for the 14 yr period were collected and used to validate hindcast model results.

A rose diagram based on the 14 yr of measurements (Fig. 1) shows that the wave climate of this region is characterized by prevailing dominant smooth and moderate sea states and by the occurrence of two different types of storms – storms from the southwest (SW – 70 % of storm occurrences) and storms from the southeast (SE – 30 % of storm occurrences).

The storm threshold for this region is defined as $H_s > 3$ m (Pessanha and Pires, 1981) which also corresponds to the mean $H_s$ of the entire 14 yr of measurements plus two times the standard deviation of the respective dataset. The minimum time duration above the storm threshold to be considered a storm is 3 h and the individualization of storm events was made through an independence criterion defined as when 30 h elapsed between consecutive $H_s$ records (Twan, 1988; Morton et al., 1997; Dorsch et al., 2008) over 3 m (the storm threshold for the region). The largest waves are from the SW, generated by deep atmospheric low pressure systems whose paths are more southerly than usual. The typical $H_s$ during SW storms is around 4 m and in general these storms occur more than once a year; however, there are events that can reach $H_s \sim 7$ m. These SW storms occur mainly during the winter (December–March).

SE storms occur when a strong "Levante" (strong Mediterranean easterly wind) is blowing from Gibraltar Strait. In contrast to the SW storms, which are related to synoptic scales, SE storms are mainly due to mesoscale atmospheric patterns. These patterns involve the Azores high extending over the Iberian Peninsula and North Africa while there is a pronounced low over northern Africa, thus generating a surface pressure gradient over the Strait that gives rise to strong winds and stormy waves (Dorman et al., 1995). These storms occur mainly between October and May and typically with $H_s < 4$ m. The maximum $H_s$ recorded during SE storms is <6 m.

## 2.2 Model data

The historical wave climate for the Faro buoy's location was hindcasted with the third-generation spectral wave model WAVEWATCH III (hereinafter referred to as WW3) (Tolman, 2009) in its version V3.14. The parameterization selected for the study is the one described and validated in Ardhuin et al. (2009).

In order to accurately simulate the wave field in the Gulf of Cadiz, a one-way nesting strategy was adopted. This semi-enclosed basin is episodically dominated by fetch-limited wind seas, due to its location partly sheltered from NW and NNW ocean swells and the presence of local winds, such as the Levante. A fine resolution grid nested in a coarser one was therefore required in order to more accurately take into account the effects of the wind and the local topography. The regional model of Dodet et al. (2010), corresponding to a 0.5° resolution coarse grid covering the North Atlantic Ocean and forced with the NCEP/NCAR reanalysis wind fields (Kalnay et al., 1996) was used to generate wave spectra along the boundaries of a finer 0.05° resolution grid extending from 10° W to 6° W in longitude and from 35° N to 38° N in latitude. In addition to this spectral forcing, the model was fed with hourly high-resolution (0.5°) wind fields, generated from the HIPOCAS project (Feser et al., 2001, Weisse et al., 2009). The spectral grid uses 24 regularly spaced directions and extends from 0.041 Hz to 0.41 Hz with 25 exponentially spaced frequencies.

A 54-yr simulation was performed for the period 1952 to 2006 and provided 3-hourly time-series of mean wave parameters at the specific location of the Faro buoy (Fig. 1). In order to deal with the very large subsequent computational cost, the Message Passing Interface (MPI) version of WW3 was used on a 268 processors Fujitsu-Siemens PC-cluster. The whole simulation was split into six 10-yr runs, each of them running on 20 processors within 30 h.

## 2.3 Model data validation

Model results were validated through comparisons with coincident measurements from Faro buoy. A linear correlation of the entire coincident $H_s$ data was analysed through two

**Table 1.** Model validation results (1995–2006).

| Storm characteristics | | | |
|---|---|---|---|
| | Measured | Model | Prediction parameters (%) |
| Number of storms | 91 | 85 | 93 % |
| Number of days with storms | 163 | 149 | 91 % |

| Wave Height | | |
|---|---|---|
| | $r^2$ (Measured vs Model) | RMS (Measured − Model) |
| 99.8th Percentile | 0.77 | 0.42 m |

statistical indicators: coefficient of determination ($r^2$) and root mean squared error (RMSE) of the fit. Other comparisons between model and measurements were made using other storm parameters investigated in this study namely, the annual number of storms, the annual number of days with storms, and the annual 99.8th $H_s$ percentile ($H_{s99.8}$).

The comparisons of the first two storm characteristics (annual number of storms, annual number of days with storms) were evaluated through a prediction parameter, which represents the percentage of events that were correctly predicted by the model. The quality of the extreme wave percentile ($H_{s99.8}$) was assessed through the $r^2$ coefficient from the linear fitting between the model and measured data. The RMSE between measured and model extreme wave percentiles was also calculated to indicate the average mismatch between each result obtained from the measurements and the model data. The correlation between model data and coincident measurements from Faro buoy indicates that the $H_s$ model results present a good agreement for the majority of the compared data (Fig. 2a), with an $r^2$ of 0.74 and a fit RMSE of 36 cm.

Comparisons of the annual number of storms and of the annual number of days with storms also present a good agreement between model and measurements, with the prediction parameter having values above 90 % (Table 1; Fig. 2b and c). These results also show that in both cases the model underestimates the measurements. The comparison using the extreme wave height percentile ($H_{s99.8}$) shows the same order of quality, presenting $r^2$ of 0.77 and RMSE between model data and measurements of 0.42 m (Table 1). Through these results, it is also possible to verify that the model seems to slightly overestimate (by <20 %) the predicted values of $H_{s99.8}$ compared to the measurements (Fig. 2d).

The two datasets (measured and modelled) were combined by concatenating the modelled data to the measured dataset
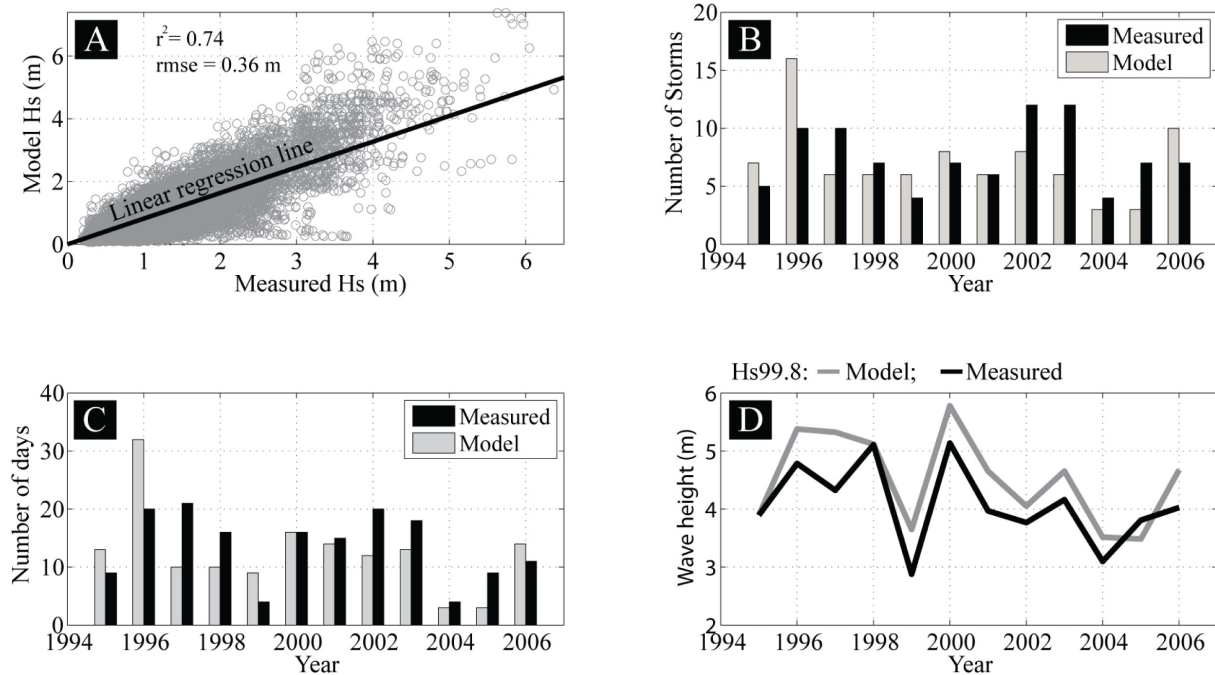
**Fig. 2.** Model validation results; **(A)** linear regression between model and measured data; **(B)** comparison of the annual number of storms between model and measurements; **(C)** comparison of the annual number of days with storms between model and measurements; **(D)** comparison of annual 99.8 percentile between model and measurements.

to create a single dataset covering the period January 1952 to December 2009. The presented modelling strategy was able to generate a historical wave dataset of comparable quality to previous studies of wave hindcasting for the Atlantic Ocean (e.g. Swail et al., 2000), and for the same area from the HIPOCAS project (Pilar et al., 2008).

## 3   Analysis of historical storminess

The duration and frequency of storms were investigated through the calculation of the annual number of days with storms and the annual number of storms for the entire dataset. Storm duration characteristics were also assessed through the calculation of the maximum and mean annual individual storm event durations.

Storm wave heights were analysed through the computation of the annual $H_{s99.8}$. Many previous investigations (e.g. Wang and Swail, 2000; Matulla et al., 2007) use the 99th percentile to assess extreme wave height variability. However, in this study, a preliminary analysis of the entire dataset indicated that in some years the annual percentage of occurrence of storms is below 0.5 %, which means that to properly characterize the annual variability of storm occurrence, a higher percentile is required. After some testing with different percentiles, it was found that the $H_{s99.8}$ was the best percentile with which to characterize annual storm variability, since for

almost all the years the calculated wave heights were above the storm threshold (3 m).

Long-term (57 yr) trends were calculated through the fit of a linear regression of the storm parameters (annual number of storms; annual number of days with storms; maximum and mean annual individual storm durations; and annual $H_{s99.8}$) on time (years). From each fit, the signal of the trend (positive or negative regression slope) and the yearly rate (value of regression slope) were calculated for each storm parameter. The statistical significance of each result was inferred with respect to the 0.01 and 0.05 levels, using the Pearson correlation coefficient.

For three storm parameters (annual number of storms, annual number of days with storms, and annual $H_{s99.8}$), the pattern of variation was also analysed by smoothing the annual values using a 3-point moving average and fitting a sum of sine functions to each set of moving average values to provide a visual representation of the smoothed data. To compute the relationships between the smoothed storm parameters, the moving averaged datasets were normalized (between 0 and 1).

Quantification of the relationships between all the storm parameters was made through linear regression using the raw data for each pair of parameters. Correlation significance levels were inferred with respect to the 0.01 and 0.05 levels, using the Pearson correlation coefficient. The North Atlantic Oscillation (NAO) index was the parameter most commonly

**Table 2.** Storm parameters and extreme wave height percentile trends.

| Parameter | $R^2$ | Trend |
|---|---|---|
| Annual number of storms | 0.008 | 0.01; 0.8 (storms yr$^{-1}$; total) |
| Annual number of days with storms | 0.005 | 0.03; 1.45 (days with storm yr$^{-1}$; total) |
| Annual maximum storm duration | −0.002 | −0.003; 0.2 (days yr$^{-1}$; total) |
| Annual mean storm duration | 0.0001 | 0.0003; 0.02 (days yr$^{-1}$; total) |
| $H_{s99.8}$ | −0.01 | −0.005; −0.27 (m yr$^{-1}$; total) |

used to explain phases of enhanced and reduced storminess along European Atlantic coastlines (Kushnir et al., 1997; Wang et al., 2003; Lozano et al., 2004; Matulla et al. 2007; Dodet et al., 2010). Positive values of the index can be generally associated with more storms approaching Northern Europe, while stormy conditions in Southern Europe would be attributed to negative index values. The correlation between the NAO index (monthly averaged difference of normalized sea level pressure (SLP) between Lisbon and Stykkishol-mur/Reykjavik; Hurrell, 1995) and storm wave heights was explored using four datasets and two different comparisons: (1) annual mean NAO index vs. Annual $H_{s99.8}$; Smoothed annual mean NAO index vs. Smoothed annual $H_{s99.8}$; (2) Winter mean NAO index vs. Winter $H_{s99.8}$; Smoothed winter mean NAO index vs. Smoothed winter $H_{s99.8}$.

Regarding winter values of the parameters, several authors suggest that the wave climate winter season corresponds to the months between December and March (e.g. Bauer, 2001; Dodet et al., 2010). However, our preliminary tests indicated that March presents a very low percentage of storm occurrences. For this reason it was decided that the winter season for the present analysis should be between December and February.

The correlations for annual/winter periods between the NAO index and $H_{s99.8}$ were computed using the raw and smoothed data, with the latter computed through a three-point moving average of the raw data.

SE storms, due to their regional scale forcing (Dorman et al., 1995), cause a weakening of the correlations between the NAO index and $H_{s99.8}$ as preliminary tests indicated. For this reason, SE storms were excluded from this correlation analysis, and therefore the NAO analysis is valid only for SW storms. The statistical significance of each correlation was also analysed against the 0.01 and 0.05 significance levels.

## 4 Results

### 4.1 Historical storminess trends

Linear regression models relating each of the storm parameters and extreme wave height percentile to time are not statistically significant and have very low $R$-square values

(Table 2). Therefore, none of the storm and wave parameters shows a significant linear trend when assessed over the entire computed period.

### 4.2 Storm parameters: variability and relationships

The year with the maximum number of storms was 1963 and the minimum 1954 (Fig. 3a). Results also show that the period 1952 to 1965, despite these storm frequency maximum and minimum, was a very stable period with a yearly average of 5 storms (Fig. 3a). The period between 1973 and 1988, despite some positive peaks, presented the lowest annual average number of storms, with many years having less than 3 storms (Fig. 3a). From 1989 until 2005, the smoothed line indicates a well-defined sinusoidal behaviour of storm occurrence, with peaks in/around 1989, 1996, and 2001, and troughs in/around 1993, 1999, and 2005.

The years with the maximum and minimum values of number of days with storms are coincident with the years that were found for the maximum and minimum values for the annual number of storms, 1963 and 1954, respectively (Fig. 3b). Beyond this, the pattern of variability of number of storm days was found to be very similar to that found for the annual number of storms. The sinusoidal behaviour for the smoothed line between 1989 and 2005 is even more apparent for the number of days with storms, since the troughs between peaks are deeper (Fig. 3b). The troughs of these cycles seem to be in phase with the troughs found for the annual number of storms (Fig. 3b).

The annual maximum individual storm duration presents a maximum value in both 1958 and 1972 (6 days duration each – Fig. 3c). The maximum value of the annual mean individual storm duration (three days) was in 1970 (Fig. 3c). The minimum values of these storm parameters occur in many years and for that reason they are not exhaustively described in the text. Results also show that peaks of the annual mean individual storm duration occur almost every time there are peaks in the annual maximum individual storm duration (Fig. 3c). During the period from 1952 to 1982, the maximum individual storm duration exceeded four days only during five years (1952, 1958, 1970, 1972, and 1981); while from 1982 and on this value was exceeded twice (in 1998 and 2009) (Fig. 3c).
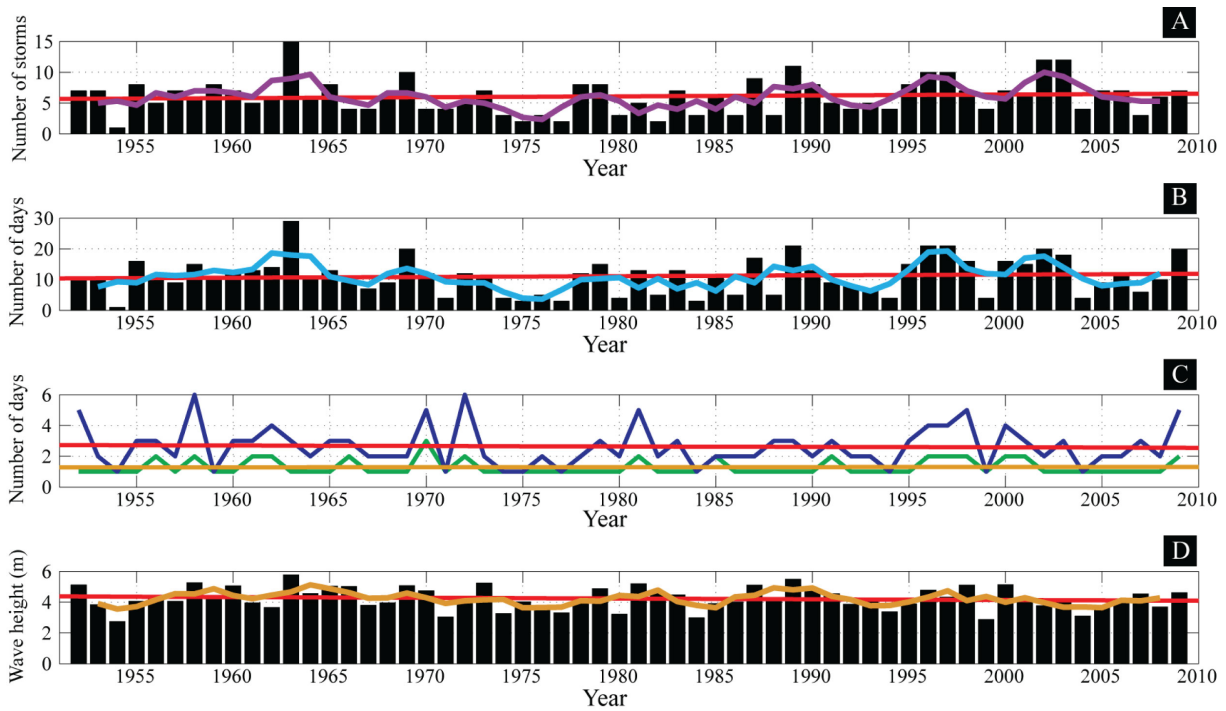
**Fig. 3.** Variations in annual storm parameters and extreme wave height percentile. Legend: **(A)** annual number of storms (black bars), moving average data (3 points – purple curve) and linear regression line (red line); **(B)** annual number of days with storms (black bars), moving average data (3 points – blue curve) and linear regression line (red line); **(C)** annual maximum individual storm duration (blue curve), annual mean individual storm duration (green curve), annual maximum individual storm duration linear regression line (red line) and annual mean individual storm duration linear regression line (brown line); **(D)** annual $H_{s99.8}$ (black bars), moving average data (3 points – brown curve) and linear regression line (red line).
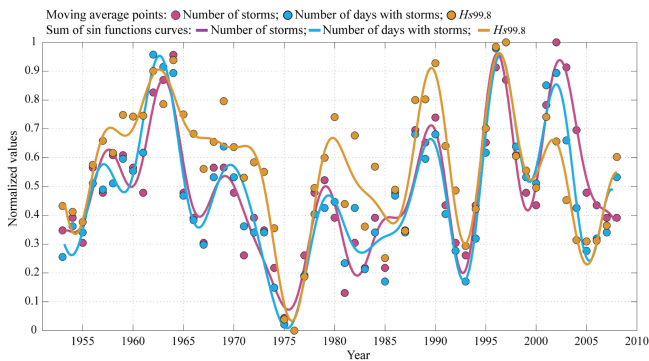


**Fig. 4.** Normalised and smoothed annual storm parameters and $H_{s99.8}$. A sum of sin functions is fitted to each variable.

The maximum value of annual $H_{s99.8}$ of ∼ 6 m was in 1963, which coincides with the occurrence of the maximum values for both the annual number of storms and annual number of days with storms (Fig. 3a and b). The minimum value of $H_{s99.8}$ of 2.7 m was in 1954 (Fig. 3d), which coincides with the occurrence of the minimum values for both the annual number of storms and annual number of days with storms (Fig. 3a, b and d).

The overlapping of the smoothed annual storm parameters (Fig. 4) indicates that the annual number of storms and the annual number of days with storms present very good agreement in terms of phase of variation. Both of these storm parameters follow a sinusoidal pattern of variation with time, showing a difference between peaks of about 7–8 yr (Fig. 4).

Annual $H_{s99.8}$ variations show small differences in phase from the other two storm parameters, showing good agreement in phase until the peak of 1963. Between 1965 and 1973 and between 1982 and 1987, the variations underwent phase deviations. The most recent years show an increase of annual number of days with storms and $H_{s99.8}$ trending to another peak. However, the annual number of storms is trending to lower values (Fig. 4).

Linear regression was performed for all bivariate combinations of storm parameters, with only the significant results portrayed in Fig. 5. The highest correlation was obtained between the annual number of storms and annual number of days with storms (Fig. 5a) with an $r^2$ of 0.82. This result confirms the pattern observed in Fig. 4. There are also significant correlations between $H_{s99.8}$ and the annual number of storms and days with storms (Fig. 5b and c). Another significant correlation was also obtained between the annual maximum and the mean individual storm duration parameters with an $r^2$ of 0.47 (Fig. 5d), although the precision of
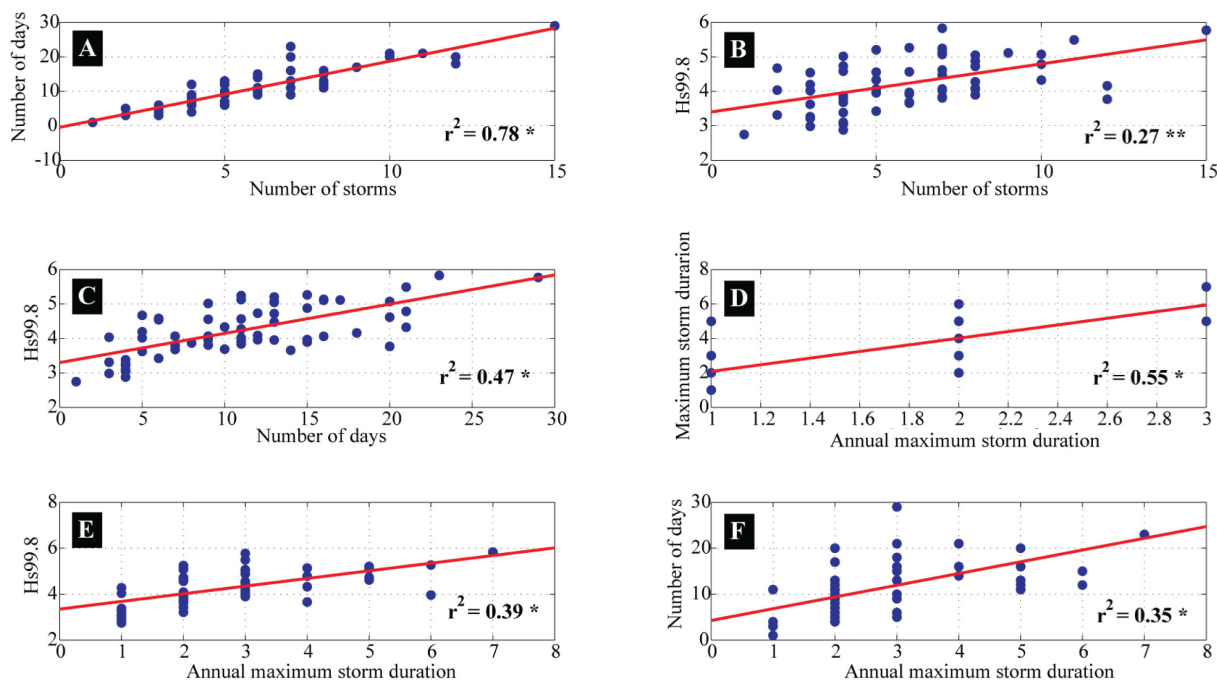
**Fig. 5.** Dispersion diagrams showing the correlations between storm parameters; **(A)** annual number of storms vs. annual number of days with storms; **(B)** annual number of storms vs. annual $H_{s99.8}$; **(C)** annual number of days with storms vs. annual $H_{s99.8}$; **(D)** annual maximum individual storm duration vs. annual mean individual storm duration; **(E)** annual maximum individual storm duration vs. annual $H_{s99.8}$; **(F)** annual maximum individual storm duration vs. Annual number of days with storms. * significant for $p < 0.01$; ** significant for $p < 0.05$.

the data (daily) limit the effectiveness of this result. Both the annual number of days with storms and the annual $H_{s99.8}$ present low but significant, correlations with annual maximum individual storm duration, with values of $r^2$ of 0.34 and 0.3, respectively (Fig. 5e and f).

### 4.3 Historical storminess and NAO

The correlations between the NAO index and $H_{s99.8}$ show that different results are obtained for linear regression when calculated for the two different datasets of annual data and winter data (Table 3). The correlation ($-0.37$) using the winter dataset is significant, whereas that using the annual dataset is not. When the correlations are established with winter datasets, the results are better than with the annual datasets (Table 3). The closer relationship is also seen when comparing Fig. 6a (annual) with Fig. 6b (winter). Winter NAO index variations for the analysed period show a negative phase between the early 1950s and the beginning of the 1970s (Fig. 6). After this negative phase, the winter NAO index presents a more sinusoidal behaviour. For the same periods, winter $H_{s99.8}$ exhibits a variation pattern almost inverse to that of the winter NAO index (Fig. 6b).

**Table 3.** NAO index and extreme wave height percentile correlations, using different periods (Annual, Winter).

| Dataset | Annual NAO index vs. Annual $H_s99.8$ ($r^2$) | Winter NAO index vs. Winter $H_s99.8$ ($r^2$) |
|---|---|---|
| Raw data | $-0.05$ | $-0.18$ |
| Moving average (3 points) | $-0.12$ | $-0.37$ * |

* significant for $p < 0.01$.

## 5 Discussion

### 5.1 Historical storminess trends

Previous studies indicate that cyclonic activity and wave heights in the northern part of the North Atlantic have been increasing between 1953 and 2009 (Serreze et al., 1997; Graham and Diaz, 2001; Geng and Sugi, 2001; Gulev et al., 2001; Wang et al., 2006; Dodet et al., 2010), and that wave heights in the mid to lower latitudes of the North Atlantic have been decreasing between 1942 and 2009 (Kushnir et al., 1997; Wang and Swail, 2000; Swail et al., 2000; Wang et al., 2003; Dodet et al., 2010). At a European level and
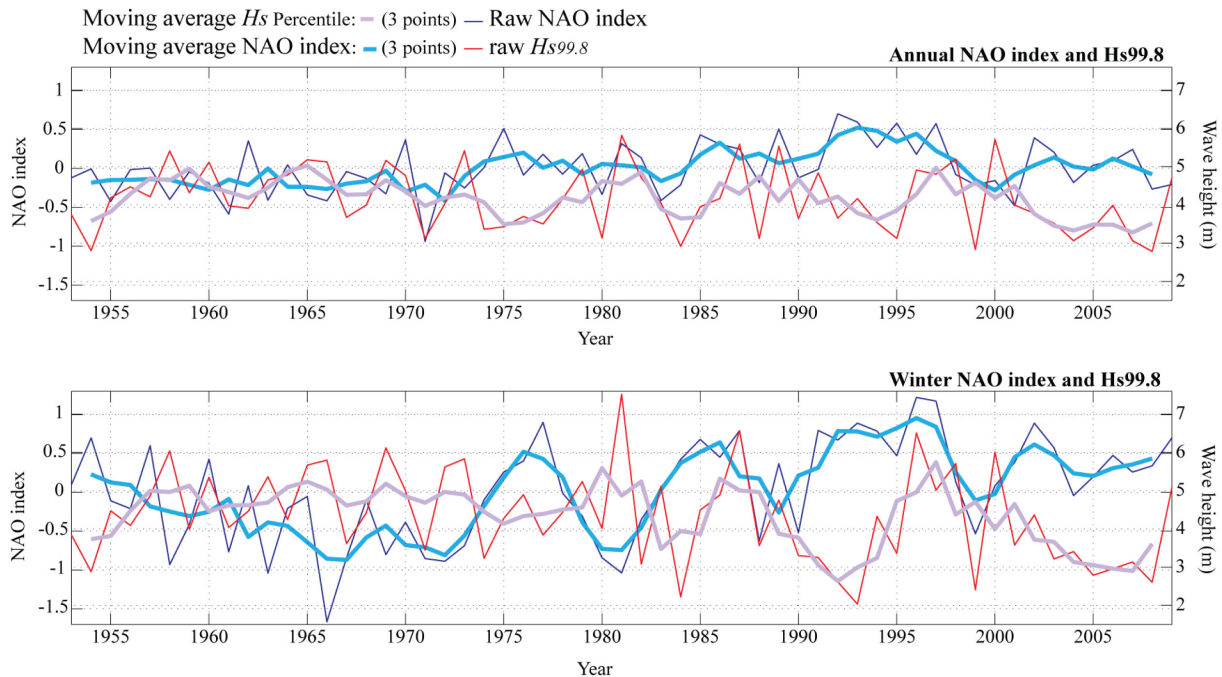
**Fig. 6.** NAO index versus $H_{s99.8}$ using annual (**A**) and winter (**B**) data.

through a group of independent regional analysis of several storm parameters (duration, intensity, and frequency), Ferreira et al. (2009) concluded that there is no general trend (either increasing or decreasing) in storminess between 1948 and 2009.

The analysis of overall data trends in the present study reveals that none of the storm parameters analysed shows a significant increase or decrease over the period of interest, which is in agreement with the findings of Ferreira et al. (2009). Presented results sometimes differ from other previous studies (e.g. Kushnir et al., 1997; Wang and Swail, 2000; Swail et al., 2000; Wang et al., 2003; Dodet et al., 2010), probably due to factors such as different modelling strategies used (e.g. resolution of wind fields and model grids), different dataset lengths, and different wave height parameters analysed. For instance, Kushnir et al. (1997) analysed monthly average significant wave heights using a smaller hindcast dataset (only 10 yr) with smaller (5 times) grid resolution. Wang and Swail (2000), Swail et al. (2000), and Wang et al. (2003) also used smaller wave field resolution and broader computational grids to generate a 40-yr-long (1958–1997) wave dataset. The generated dataset allowed historical trends to be identified in the mean significant wave height, and the 90th and 99th height percentiles for the entire North Atlantic but doesn't incorporate measurements at specific points. Dodet et al. (2010) used the same wind forcing as the present study and a computational grid with 0.5° resolution to generate a 57-yr hindcast (1953–2009) wave dataset. The historical trends in the annual 90th

percentile of significant wave height were investigated in that study for the entire North Atlantic region. The results from the above-mentioned previous studies converge to a significant decreasing in all wave height indicators along the mid and lower latitudes of the North Atlantic, including the region of our study area. The present study also shows a negative signal in the trend of $H_{s99.8}$, but with the absence of statistical significance.

Two main differences between our study and previous investigations were the forcing of a high resolution wind field (0.5°) from the HIPOCAS project and the inclusion of a high resolution (0.05°) nested grid covering the south of Portugal and Cadiz Gulf. Through the modelling strategy used, the local wave forcing was better reproduced than in previous studies (Pilar et al., 2008), resulting in an improved historical wave dataset. In addition, the study used the higher resolution computational nested grid which allowed a more satisfactory representation of wave propagation along this region. This point is important since the south of Portugal is physically sheltered from the main source of storm swell coming from the North of the North Atlantic. The present study also includes measurements of wave heights (14 yr) to validate the hindcast and to complement the analysed dataset.

Another potential cause for differences in trends between this study and previous investigations are the wave height indicators used. This study uses an annual wave height percentile (99.8 %) that was chosen (based on measurements) in order to better characterize the wave heights above the storm threshold (3 m) of the study region. Through the exploratory

analysis of the entire dataset, it was possible to identify that for some years, storms ($H_s > 3$ m) accounted for less than 0.5 % of the observed waves. This means that even a 99th percentile cannot be adequately used to assess the trends of the wave heights above the storm threshold and that percentiles such as 90th are not representative of storm conditions. The prior knowledge of storm wave thresholds in each study area contributes to define and use the most appropriate wave height percentile to characterise storms, which may not always have been the case in previous investigations (generic for the entire North Atlantic, for instance). Therefore the prior definition of a storm threshold is fundamental to the development of a historical storminess analysis. The use of different storm thresholds could mean the characterization of different meteorological events which can even have no relation with a storm event.

## 5.2 Storm parameters: variability and relationships

The clearest pattern that can be observed in the storm parameter results is the oscillatory behaviour that all parameters present with time (Fig. 4). Years with peaks of high values followed by troughs of minimum values with a 7–8 yr timescale are clearly identified (Fig. 4), and they are in agreement with patterns that have been observed in previous studies (e.g. WASA, 1998; Matulla et al., 2007; Ferreira et al., 2009).

Detailed comparison of storm parameters variability between the present results and previous findings indicate that the decline in all storm parameters from the early 1960s to the mid-1970s and the increase between the 1970s and 1980s is in agreement with the findings of prior investigations (e.g. Davis et al., 1993; WASA, 1998; Ferreira et al., 2009). Also, as it was verified in previous studies (e.g. WASA, 1998; Ferreira et al., 2009), the magnitude of the variations are comparable throughout the time series. Thus, despite the clear pattern of cyclic variations, the variability of the storm parameters has not changed significantly over time. This finding suggests that the observed amounts of variation and the cyclic behaviour may be expected to continue into the near future.

The bivariate correlations between storm parameters indicate that storm frequency and duration are highly correlated, with the annual number of storms and days with storms presenting the strongest relationship. The correlations between these two parameters and the storm duration parameters (maximum and mean storm duration) were, however, weak. Considering that the annual number of days with storms and $H_{s99.8}$ are positively correlated, and that these two parameters have significant positive correlations with the maximum individual storm duration, it seems that years with a higher number of stormy days have a high probability of presenting higher energy peaks (high $H_{s99.8}$ value) and, to a smaller extent, a higher maximum individual storm duration.

## 5.3 Storminess and the NAO

Results from the correlations between $H_{s99.8}$ and the NAO index show that these two variables are correlated only when the winter season datasets are used. This is in agreement with Bauer's (2001) findings, which show that wave height is considerably better correlated with the winter NAO index than with the annual (whole) dataset for the NAO index. However, a significant (but low) correlation was found when the raw data were smoothed through a moving average. These results are in agreement with those of Dodet et al. (2010), in which a similar correlation coefficient between the winter NAO index and winter $H_{s90}$ was found for the same region. Our findings indicate that the NAO index explains only a small part of the $H_{s99.8}$ storm wave height variation in this region. Matulla et al. (2007) have previously shown that the NAO index is not very helpful in accounting for storminess in central Europe. Alexandersson et al. (1998) also found that the NAO index fails to explain storminess in NW Europe.

The capacity of the NAO index to explain storminess across Europe varies spatially and according to the particular period under consideration (see Matulla et al., 2007; Ferreira et al., 2009). However, the results obtained in this investigation indicate that the NAO index is not able to explain much of the storm wave height variability for South Portugal. This is probably due to regional characteristics (e.g. influence from regional storms generated at the Gulf of Cadiz, sheltering from the North Atlantic stormy waves) that have an important influence on the definition of the annual storm wave climate. This suggests that further research is needed in order to understand the driving factors of storm climate of this region above and beyond the influence of the NAO.

## 6 Conclusions

This study investigated historical variations and trends in storminess for the coast in the South of Portugal for the period 1952 to 2009 using both measured and modelled data. No statistically significant linear trend (either a decrease or increase) was found for any of the storm characteristics (wave height, storm duration, and number of storms) over the period of interest. The main pattern of historical storminess variability is an oscillatory variability in storm parameters, with peaks every 7–8 yr on average, with the magnitude and style of variation found in recent years being similar to that further in the past. Years with a higher number of stormy days generally have higher wave heights and higher maximum individual storm durations.

The results also reveal that the NAO index is able to explain only a small amount of the annual variability of storm wave height or storm frequency in this region. Future work should include other climatic factors, in addition to the NAO index, to explain the annual storminess variability in the South of Portugal, a setting in which local factors may prove

to be the significant drivers of variation in storminess. A large set of regional studies such as the one detailed in this paper should be performed in order to obtain a wide representation of variation in storminess, and to identify the drivers of the variation, including a better understanding of local and regional effects.

Edited by: J. A. Jimenez
Reviewed by: E. Mendoza and another anonymous referee

# References

Alexander, L. V., Tett, S., and Jonsson, T.: Recent observed changes in severe storms over the United Kingdom and Iceland, Geophys. Res. Lett., 32, L13704, doi:10.1029/2005GL022371, 2005.

Alexandersson, H., Schmith, T., Iden, K., and Tuomenvirta, H.: Long-term trend variations of the storm climate over NW Europe, The Global Atmosphere and Ocean System 6, 97–120, 1998.

Ardhuin, F., Marié, L., Rascle, R., Forget, P., and Roland, A.: Observation and estimation of Lagrangian, Stokes and Eulerian currents induced by wind and waves at the sea surface, J. Phys. Oceanogr., 39, 2820–2838, 2009.

Bacon, S. and Carter, D. J. T.: Wave climate changes in the north Atlantic and North Sea, Int. J. Climatol., 11, 545–558, 1991.

Bauer, E.: Interannual changes of the ocean wave variability in the North Atlantic and in the North Sea, Clim. Res., 18, 63–69, 2001.

Davis, R. E., Dolan, R., and Demme, G.: Synoptic climatology of Atlantic coast extratropical storms, Int. J. Climatol., 13, 171–189, 1993.

Dodet, G., Bertin, X., and Taborda, R.: Wave climate variability in the North-East Atlantic Ocean over the last six decades, Ocean Model., 31, 120–131, 2010.

Dolan, R., Lins, H., and Hayden, B.: Mid-Atlantic coastal storms, J. Coastal Res., 4, 417–433, 1989.

Dorman, C., Beardsley, R., and Limeburner, R.: Winds in the Strait of Gibraltar, Quart. J. Roy. Meteorol. Soc., 121, 1903–1921, 1995.

Dorsch, W., Newland, T., Tassone, D., Tymons, S., and Walker, D.: A statistical approach to modelling the temporal patterns of ocean storms, J. Coastal Res., 24, 1430–1438, 2008.

Ferreira, Ó., Vousdoukas, M. V., and Ciavola, P.: MICORE Review of Climate Change Impacts on Storm Occurrence, (Open access, Deliverable WP1.4), 2009.

Feser, F., Weisse, R., and von Storch, H.: Multi-decadal atmospheric modelling for Europe yields multi-purpose data, EOS Transactions, 82(28), 305–310, 2001.

Geng, Q. and Sugi, M.: Variability of the North Atlantic cyclone activity in winter analysed from NCEP-NCAR reanalysis data, J. Climate, 14, 3863–3873, 2001.

Graham, N. E. and Diaz, H. F.: Evidence for intensification of North Pacific winter cyclones since 1948, B. Am. Meteorol. Soc., 82, 1869–1893, 2001.

Grigorieva, V. and Gulev, S.: Extreme wind waves worldwide from the VOS data and their changes over the last 50 years, Proceedings of 9th International Workshop on Wave Hindcasting and Forecasting, September Victoria, British Columbia, Canada, 24–29, 2006.

Gulev, S. K., Zolina, O., and Grigoriev, S.: Extratropical cyclone variability in the Northern Hemisphere winter from the NCEP/NCAR Reanalysis data, Clim. Dynam., 17, 795–809, 2001.

Hurrell, J. W.: Decadal trends in the North Atlantic Oscillation: regional temperatures and precipitations, Science, 269, 676–679, 1995.

Kalnay, E., Kanamitsu, M., Kistler, R., Collins, W., Deaven, D., Gandin, L., Iredell, M., Saha, S., White, G., Woollen, J., Zhu, Y., Leetmaa, A., Reynolds, B., Chelliah, M., Ebisuzaki, W., Higgins, W., Janowiak, J., Mo, K. C., Ropelewski, C., Wang, J., Jenne, R., and Joseph, D.: The NCEP/NCAR 40-Year Reanalysis Project, B. Am. Meteorol. Soc., 77, 437–472, 1996.

Kushnir, Y., Cardone, V. J., Greenwood, J. G., and Cane, M. A.: The recent increase in North Atlantic wave heights, J. Clim., 10, 2107–2113, 1997.

Lozano, I., Devoy, R. J. N., May, W., and Andersen, U.: Storminess and vulnerability along Atlantic coastlines of Europe: analysis of storm records and of a greenhouse gases induced climate scenario, Mar. Geol., 201, 205–225, 2004.

Matulla, C., Schöner, W., and Alexandersson, H.: European storminess: late nineteenth century to present, Clim. Dynam., 31, 125–130, 2007.

Morton, I. D., Bowers, J., and Mould, G.: Estimating return period wave heights and wind speed using a seasonal point process model, Coast. Eng., 31, 305–326, 1997.

Pessanha, L. and Pires, O.: Elementos sobre o clima de agitação marítima na costa Sul do Algarve, Report Instituto de Meteorologia, 67 pp., 1981.

Pilar, P., Soares, C. G., and Carretero, J. C.: 44-year wave hindcast for the North East Atlantic European coast, Coast. Eng., 55, 861–871, 2008.

Schwartz, M. L.: Encyclopedia of Coastal Science. Springer, Dordrecht, Netherlands, 2005.

Serreze, M. C., Carse, F., Barry, R. G., and Rogers J. C.: Iceland low cyclone activity: Climatological features, linkages with the NAO, and relationships with the recent changes in the Northen Hemisphere circulation, J. Climate, 10, 453–464, 1997.

Swail, V. R., Ceccacci, E. A., and Cox, A. T.: The AES40 north Atlantic wave reanalysis validation and climate assessment, 6th International Workshop on wave hindcasting and forecasting, Monterey, California, USA, 2000.

Tawn, J. A.: An extreme-value theory model for dependent observations, J. Hydrol., 101, 227–250, 1988.

Tolman, H. L.: User manual and system documentation of WAVE-WATCH III version 3.14, NOAA/NWS/NCEP/MMAB Technical Note 276, 194 pp., 2009.

WASA: Changing waves and storms in the northeast Atlantic, B.

Am. Meteorol. Soc., 79, 741–760, 1998.

Wang, X. L. and Swail, V. R.: Changes of extreme wave heights in Northern hemisphere oceans and related atmospheric circulation regimes, J. Climate, 14, 2204–2221, 2000.

Wang, X. L. and Swail, V.: Trends of atlantic wave extremes as simulated in a 40-yr wave hindcast using kinematically reanalyzed wind fields, J. Climate, 15, 1020–1035, 2001.

Wang, X. L., Zwiers, F. W., and Swail, V. R.: North Atlantic ocean wave climate change scenarios for the twenty-first century, J. Clim., 17, 2368–2383, 2003.

Wang, X. L., Swail, V. R., and Zwiers, F. W.: Climatology and changes of extratropical cyclone activicty: comparison of ERA-40 with NCEP-NCAR reanalysis for 1958–2001, J. Climate, 19, 3145–3166, 2006.

Weisse, R., von Storch, H., Callies, U., Chrastansky, A., Feser, F., Grabemann, I., Guenther, H., Pluess, A., Stoye, T., Tellkamp, J., Winterfeldt J., and Woth, K.: Regional meteorological-marine reanalyses and climate change projections: Results for Northern Europe and potentials for coastal and offshore applications, B. Am. Meteorol. Soc., 90, 849–860, 2009.